Journal of Innovative Technology, Vol. 7, No. 1, pp. 59-66, March 2025
http://doi.org/10.29424/JIT.202503_7(1).0006

Deterministic numerical investigation for bioconvection in MHD hybrid Nanofluidic model with stretching sheet and buoyancy

Irshad Ali [1], Muhammad Asif Zahoor Raja [2*]

ABSTRACT

The bioconvective investigation characteristics of magnetohydrodynamic hybrid nano-fluid (MHD-HNF) flow comprising colloidal nanoparticles of MgO-Cu fleeting through an extending porous sheet is presented numerically with state-of-the-art computing methodologies. The study consisting of analysis of MHD-HNF flow dynamics by considering the physical elements such as Eckert number , heat generation, viscous dissipation, buoyancy influences, along with the assimilation of microorganisms contributing while water serves as base fluid and observe the impact heat generation and temperature on fluid flow in the presence of colloidal. Mathematical partial differential system of equations (PDEs) is simplified into an ordinary differential equation (ODE) system through the use of non-dimensional parameters and similarity transformations, and solution dynamic data is generated with Adams numerical method as well as the backward differentiation formula (BDF) method. Numerical solution provides discrete set of values correspond to governing parameters. The comparative studies of the outcomes from both Adams and BDF methods are converted exhaustively for further investigations of the findings. Additionally, through absolute error and solution graph the entire graphical analysis is compared. The results of absolute error and solution dynamics established a strong agreement with previously published research outcomes for the parametric investigation, physical factors effects such as velocity, temperature, concentration and microorganisms. Mutual influences are illustrated using visual depiction, while comparative numerical results are provided in sufficient number of tabular forms.

Keywords: Magnetohydrodynamic, Hybrid nano fluid, Adams numerical method, Backward Differentiation Formula, Microorganisms.

NOMENCLATURE

ODEs: Ordinary (standard) differential equations
PDEs: Partial differential equations
MHD: Magnetohydrodynamic
MRFs: magnetorheological fluids
BDF: Backward Differentiation Formula
M: parameter of magnetic field
K_P: porosity factor
p_r: non-dimensional Prandtl number
E_c: non dimensional Eckert number,
λ: buoyancy parameter
K_c: parameter of chemical reaction

1. INTRODUCTION

The configuration of a stretching sheet is commonly encountered in practical engineering challenges. It has attracted considerable attention from researchers. This is due its extensive applicability in various fields. These fields include aerospace, acoustics, glass blowing and paper manufacturing. The relevance of this configuration spans a wide range of engineering applications. When a sheet made of incompressible materials stretches linearly, its thickness decreases proportionally with the distance. This behavior is due to the material's incompressibility, which means that as the sheet stretches, its volume remains constant. Consequently, the increase in length must be accompanied by a decrease in thickness. Thus, a linear relationship can be observed between the stretching distance and the reduction in thickness. Stretching speed also related linearly with the distance. Viscous-nanofluid flow for a constantly moving sheet with a uniform speed in a quiescent medium has been studied for the oxides of aluminum, titanium, and iron-like Al2O3, TiO2, and Fe_3O_4 in water base fluid [1]. Mass and heat transfer for a power-law across a thin layer of fluid on time dependent stretching surface has been studied[2].

The study also explored the stability of magnetorheological fluids (MRFs), which are composed of iron particles suspended in silicone oil, using silica nanoparticles as a thixotropic stabilizer [3]. In binary mixtures, when colloidal particles are distributed, a layer of adsorption develops on their surface. This layer can act as a nano-scale reactor, facilitating the production of nanocrystalline materials [4].Scientific findings suggest that hybrid nanofluids outperform single nanofluids in heat transfer enhancement making them particularly beneficial in fields such as automotive , electro-mechanical systems, manufacturing process and solar energy[5]. The use of Molten salts as heat transfer in solar power plants has been incorporated. They are also used for short time thermal energy storage. Experimental investigations show that incorporat-

Manuscript received September 17, 2024; revised November 7, 2024; accepted November 21, 2024.

1 Ph.D. Scholar, Department of Data Science and AI Applications, Graduate School of Engineering Science and Technology, National Yunlin University of Science and Technology, Taiwan.

2* Professor (corresponding author), Department of Data Science and AI Applications, Graduate School of Engineering Science and Technology, National Yunlin University of Science and Technology, Taiwan. (email: rajamaz@yuntech.edu.tw)

ing the nanoparticles into the base salt can enhance the specific heat capacity. This process involves mixing of nanoparticles with salts in a very small amount and this can also boost thermal properties of the salt [6]. An innovative approach of heat transfer in fluids has been developed. This process comprising thermophysical characteristics. These characteristics can be tailored through their base ionic fluids. This makes them highly adaptable for various applications [7].

The rheological effect upon the heat capacity of various suspensions in water as base fluid has also been studied by many researchers. The experimental findings conclude that it can enhance potential condition of the heat transfer ability of fluids. [8]. Heat transfer characteristics in absorbent surface-media also has gain much interest. Research shows that in Past decades absorbent and porous surface materials have large applications as heat transfer in various fields such as ceramic processing, catalytic reactors, heat exchangers and so on. Additionally, hybrid nanofluids have an excellent and superior heat transfer property in various porous surface materials, so that's why they are widely used in many fields [9]. Nanofluidic system and the cooling efficiency has an influence on porous media surfaces and has shown significant interest for the researchers. The natural convection process for a nanofluid having an absorbent porous matrix and a square type cavity has also been investigated [10]. Further investigations on heat transfer phenomena for a hybrid nanofluid of second grade reveal important insights for the permeable sheet [11]. The investigation examines hybrid nanofluids consisting alumina and copper nanoparticles dispersed in sodium alginate (SA) as the carrier fluid to enhance the rate of heat transfer. Additionally, thermal flow in fusion of second-grade type magnetohydrodynamic flowing nanofluid through a convective medium is explored. This study provides valuable importance and insights into the thermal characteristics of hybrid nanofluid in the MHD applications. These results explore the potential of using hybrid nanofluids to enhance heat transfer effectiveness [12]. Induction of Specific number of nanoparticles can enhance the rate of heat transfer and thermal conduction characteristics of the hybrid nanofluid [13].Heat and momentum transfer characteristics are investigated for hybrid nanofluid. Experiment shows that porous surfaces and media over a three-dimensional vertical cone impacted by different behaviors like size, shape, aspect of nanoparticles, properties of the base liquid and functioning temperature of base liquid [14].

An innovative approach is applied to different three-dimensional geometry to intensify heat generation and, in peristalsis, heat flow of magnetohydrodynamic hybrid nanofluids [15]. The numerical examination on the impacts of magnetic interaction, slip factor, and temperature change with respect to time over a spinning disk was also investigated[16].Analysis of heat transport of fluidic flow for a three dimensional cylindrical geometry is also investigated. The consequences for the magnetic force and utilizing the numerical methods in hydraulics network systems and different engineering fields is also studied [17-19]. Enhancement of thermophysical properties in hybrid nano liquid was studied by different researchers [20-24]. Hybrid nanofluids are used in many ways. They have applications in the field of microfluidics, dynamic sealing, heat generation and dissipation, and so on. Studies have shown that hybrid nanofluid flow over a flexible surface with changing viscosity is far better at the transfer of heat as compared with nanofluid of a single type of nanoparticles [25]. hybrid magnetized nanoparticles such as gold and silver in a water base liquid for a Casson hybrid nanofluid is also studied [26]. Heat, mass transfer characteristics and theoretical analysis of hydromagnetic bioconvection involving a reacting Casson nanofluid over a flexible permeable vertical superficial within a clean porous media surfaces is also studied [27].Furthermore, investigation on Casson fluidic flow mixed with gyrotactic microorganisms and motile microorganism due to an elevated surface helps to stabilize the nanofluid [28].The collective effect of thermal radiation of hybrid-nanofluid over a clean surface in Darcy-Forchheimer absorbent porous medium is also studied[29-32].Mass transfer characteristics in the existence of a chemical response in the MHD stream of a Casson fluidic flow for a porous sheet is also studied[33].The initial approximations of MHD hybrid nanofluid was refined and Adams Bash-forth method is applied to achieve highly precise and accurate numerical solutions[34].

The contributions of the current study comprise as follows:

- Investigations of the magnetohydrodynamic hybrid nanofluidic (MHD-HNF) flow with water as base fluid and MgO-Cu as hybrid-colloidal nanoparticles with the introduction of non-dimensional physical parameters are presented numerically.
- The presented study analyzes the impact of heat generation and temperature on MHD-HNF fluidic flow in the presence of colloidal nanoparticles.
- Involves partial differential system of equations simplified into ordinary differential system of equations and similarity transformations are used for the said simplification.
- The data of solution dynamics for MHD-HNF is generated viably using the Adams numerical method as well as backward differential formula and discrete values of leading parameters are obtained through numerical solutions.
- Absolute error and solution patterns are used for comparative analysis to access the effects of velocity profile, temperature, concentration and microorganisms thoroughly.

The remaining work is divided as follow: section 2 represents the mathematical formulation of MHD-HNF model, section 3 represents nonlinear solution methodology approach for the solutions of MHD-HNF model, Section 4 provides the results along with necessary interpretations, and section 5 represents the conclusions

2. MATHEMATICAL FORMULATION OF THE (MHD-HNF) MODEL

Novel MHD-HNF flow over a sheet stretched linearly through a material with permeability in two dimensions, characterized as incompressible and laminar as shown in Fig. 1. The surface of the sheet is aligned in vertical direction and stretching in horizontal direction. The research comprising, magnesium oxide (MgO) and copper (Cu) nanoparticles and water is used as base fluid. Set of equations from 1-6 represents a system of partial differential equations (PDEs) and the boundary conditions which describe the MHD-HNF model [35].

$$\left(\frac{\partial u_1}{\partial x_1}+\frac{\partial u_2}{\partial x_2}\right)=0 \quad (1)$$

$$\left(u_1\frac{\partial u_1}{\partial x_1}+u_2\frac{\partial u_1}{\partial x_2}\right)=\nu_{hnf}\frac{\partial^2 u_1}{\partial x_2^2}-\nu_{hnf}\frac{u_1}{k_r}+\frac{\sigma_{hnf}}{\rho_{hnf}}B_0^2u_1+\frac{(\rho\beta)_{hnf}}{\rho_{hnf}}g(T-T_\infty) \quad (2)$$

$$\left(u_1\frac{\partial T}{\partial x_1}+u_2\frac{\partial T}{\partial x_2}\right)=\frac{k_{hnf}}{(\rho C_p)_{hnf}}\frac{\partial^2 T}{\partial x_2^2}-\frac{1}{(\rho C_p)_{hnf}}\frac{\partial^2 q_r}{\partial x_2}+\frac{Q_0}{(\rho C_p)_{hnf}}(T-T_\infty)+$$
$$\frac{\mu_{hnf}}{(\rho C_p)_{hnf}}\left(\frac{\partial u_1}{\partial x_2}\right)^2+\frac{\mu_{hnf}}{(\rho C_p)_{hnf}}\frac{u_1^2}{k_r}+\frac{\sigma_{hnf}}{\rho_{hnf}}B_0^2u_1^2 \quad (3)$$

$$\left(u_1\frac{\partial C}{\partial x_1}+u_2\frac{\partial C}{\partial x_2}\right)=D_B\frac{\partial^2 C}{\partial x_2^2}-K_0(C-C_0) \tag{4}$$

$$\left(u_1\frac{\partial N}{\partial x_1}+u_2\frac{\partial N}{\partial x_2}\right)+\frac{bW_c}{C_h-C_\infty}\left(\frac{\partial}{\partial x_2}\left(N\frac{\partial C}{\partial x_2}\right)\right)=D\frac{\partial^2 N}{\partial x_2^2} \tag{5}$$

$$\begin{aligned}&at, x_2=0, u_1=u_h=cx_1, u_2=0, T=T_h, C=C_h, N=N_h,\\ &as, x_2\to\infty, u_1\to 0, T\to T_\infty, C\to C_\infty, N\to N_\infty\end{aligned} \tag{6}$$

Equations from 7-11 represents a system of ordinary differential equations (ODEs) accompanied by their boundary conditions.

$$f'''+ff''-\frac{1}{a_1a_2}\left((a_1a_3M+K_p)f'-a_1a_6\lambda\theta\xi^{-1}\right)-(f')^2 \tag{7}$$

$$\begin{aligned}&a_2\left(a_5+\frac{4}{3}R\right)\theta''+a_1a_4p_r\theta'+a_1a_2E_cp_r\xi^2(f')^2+a_1Qp_r\theta\\ &+p_rE_c\xi^2(a_1a_3M+K_p)(f')^2=0\end{aligned} \tag{8}$$

$$\phi''+\frac{L_e}{a_1a_2}f\phi'-\frac{L_eK_c}{a_1a_2}\phi=0 \tag{9}$$

$$x''+\frac{L_b}{a_1a_2}fx'-p_e\left(x'\phi'+(x+\Omega)\phi''\right)=0 \tag{10}$$

$$\begin{aligned}&f'(0)=1, f(0)=0, \theta(0)=1, \phi(0)=1, x(0)=1\\ &x(0)=1, f'(\infty)=0, \theta(\infty)=0, \phi(\infty)=0, x(\infty)=0\end{aligned} \tag{11}$$

Below is the similarity equation [37]

$$\begin{aligned}&\xi=\frac{x_1}{l}, \eta=x_2\sqrt{\frac{u_h}{v_{hnf}x_1}}, u_1=u_h\frac{\partial f}{\partial\eta}(\xi,\eta),\\ &u_2=-\sqrt{cv_{hnf}}\left[f(\xi,\eta)+\xi\frac{\partial f}{\partial\xi}(\xi,\eta)\right]\\ &\theta(\xi,\eta)=\frac{T-T_\infty}{T_h-T_\infty}, \phi(\xi,\eta)=\frac{c-c_\infty}{c_h-c_\infty}\\ &x(\xi,\eta)=\frac{N-N_\infty}{N_h-N_\infty}\end{aligned} \tag{12}$$

3. SOLUTION METHODOLOGY

The proposed MHD-HNF model is solved using numerical Adams and the backward Differentiation (BDF) method. Adam's method is also known as Adams-Bash forth. These two well-known methods, are implicit and explicit multi-step numerical methods most frequently used for solving ordinary differential equations (ODEs). These methods belong to the predictor- corrector family. They are particularly effective for non-stiff ordinary differential equations (ODEs). Explicit methods are used in this context. These methods are known for their stability. Additionally, they are highly efficient. Whereas the BDF method belongs to the family of implicit methods and is commonly used for solving numerically stiff ordinary differential equations (ODEs). Stiff ODEs are distinguished by their solutions that vary slowly in some variables and rapidly in others, making them challenging for explicit methods that require very small-time steps for stability [36]. Table 1 is the complete set of all scenarios of the non-dimensional parameters of the MHD-HNF model. The physical parameters in the tabulated data set are velocity profile, thermal profile, concentration and microorganisms. The physical elements are Eckert number (Ec), heat generation(Q), porosity (Kp) and buoyancy parameter(λ) are illustrated in the table.

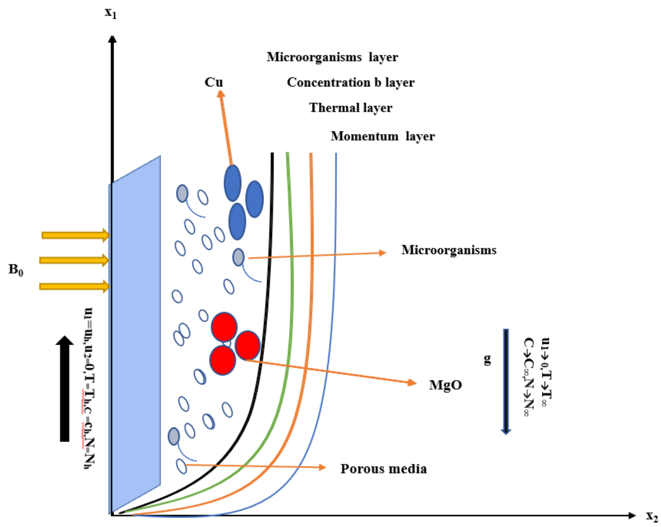

Fig. 1 Flow structure of the physical MHD-HNF model

Table 1 Parameters' variation of MHD-HNF model

Scenarios	Cases	Parameters.			
S-1	1	1.0	0.11	0.1	0.3
	2	0.5	0.11	0.1	0.3
	3	1.5	0.11	0.1	0.3
	4	2.0	0.11	0.1	0.3
S-2	1	1.0	0.5	0.1	0.3
	2	1.0	1.0	0.1	0.3
	3	1.0	1.5	0.1	0.3
	4	1.0	2.0	0.1	0.3
S-3	1	1.0	0.11	0.01	0.3
	2	1.0	0.11	0.02	0.3
	3	1.0	0.11	0.03	0.3
	4	1.0	0.11	0.04	0.3
S-4	1	1.0	0.11	0.1	0.1
	2	1.0	0.11	0.1	0.2
	3	1.0	0.11	0.1	0.3
	4	1.0	0.11	0.1	0.4

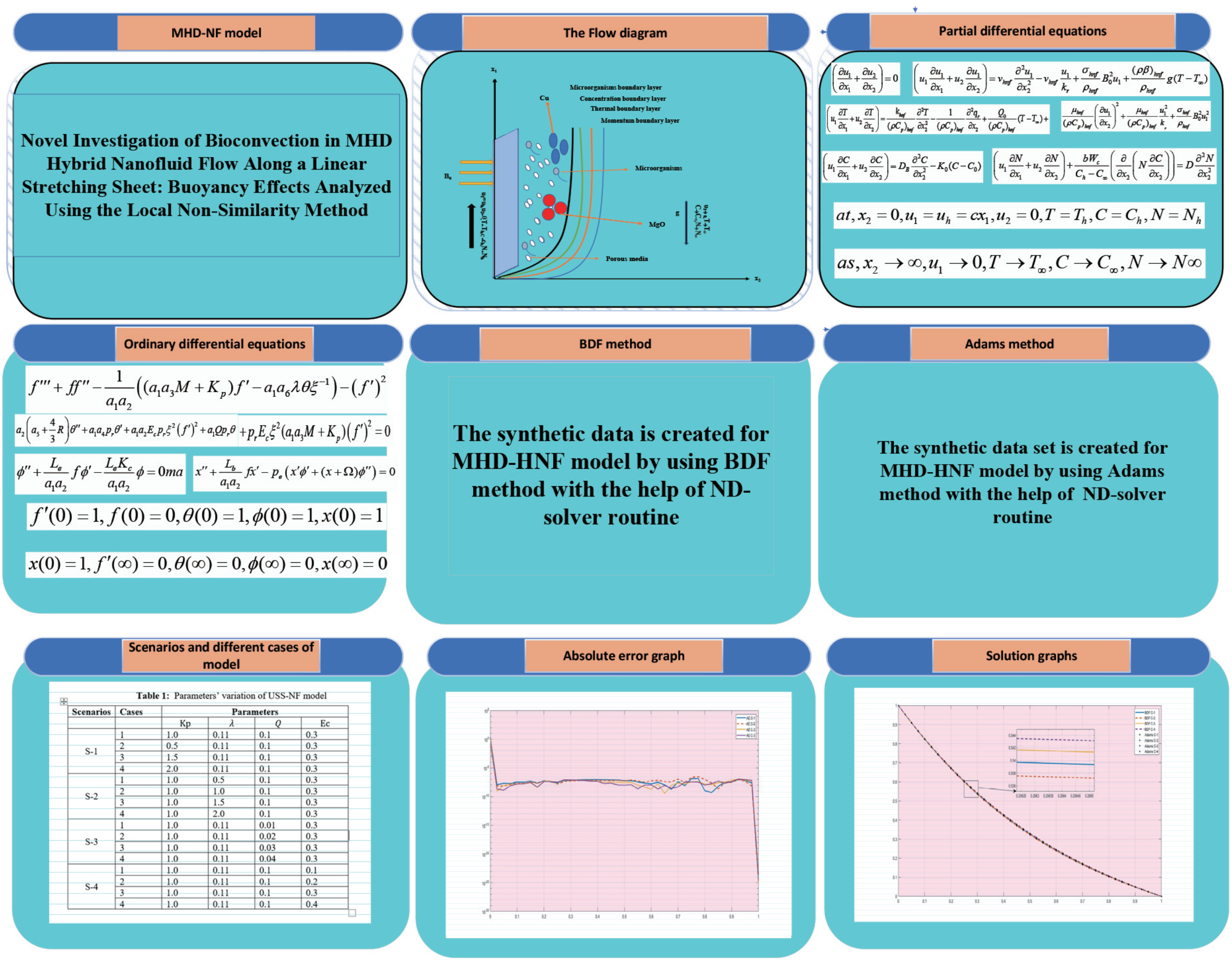

Fig. 2 Graphical abstract of the MHD-HNF model

4. RESULTS AND DISCUSSIONS

This section portrays the impact of porosity, buoyancy, heat generation, and Eckert number on velocity, temperature, concentration, and microorganisms of the MHD-HNF model. A detailed and clear analysis of a series of figures are displayed. Table 1 describes the impact variations of porosity, buoyancy, heat generation and Eckert number for different scenarios of MHD-HNF model. FiG.3-a, FiG.3-b, FiG.3-c, and FiG.3-d represents the solution graphs of velocity profile, temperature, concentration, and microorganism for SCN-01, respectively. This subsection shows the variation of porosity factor by keeping the other parameters constant. FiG.3-b, FiG.3-c, FiG.3-d shows that temperature, concentrations and microorganisms have a linear relationship by changing the porosity of the nanofluid. The FiG.3-a represents the variation of velocity profile with changing porosity of the MHD-HNF fluidic model, which exhibits almost a uniformly changing behavior and becomes flattened by increasing the porosity factor. The presence of porosity increases the resistance, which affects the speed of the fluid. In general, the porosity factor amplifies the fluid resistance, which also affects the temperature and thermal boundary layer of the MHD-HNF. FiG.4-a, FiG.4-b, FiG.4-c, and FiG.4-d represents the solution graphs of velocity profile, temperature, concentration, and microorganisms of SCN-02, respectively. The effect of the buoyancy parameter (λ) on the velocity profile is shown in FiG.4-a. The changing values of the buoyancy parameter enhance the convection currents. As a result, the temperature profile decreases, as illustrated in FiG.4-b. The consequent behavior for concentration and microorganisms for changing buoyancy parameters is portrayed in FiG.4-c and FiG.4-d respectively. FiG.5-a, FiG.5-b, FiG.5-c, and FiG.5-d represents the solution graphs of SCN-03 for the heat generation(Q) parameter, respectively. The other parameters are kept constant. Fig.5-a depicts the variation of the velocity profile by changing the heat generation of the MHD-HNF model. FiG.5-b shows the thermal variation of the MHD-HNF model with heat generation as a result thermal increase of the MHD-HNF model and as a result thermal boundary layer of the system grows. FiG.5-c and FiG.5-d represents the variations of concentration and microorganism with heat generation of SCN-03 respectively. FiG.6-a, FiG.6-b, FiG.6-c, and FiG.6-d depicts the variation of Eckert number parameter for the velocity profile, temperature profile, concentration and microorganisms of the MHD-HNF model for each case of SCN-04 respectively. Results of absolute error for MHD-HNF model is illustrated in figure.7 for velocity, temperature, concentration and microorganisms.

FiG.3-a

Solution graph outcomes

$F'[\zeta]$ → Y-axis

ζ → X-axis

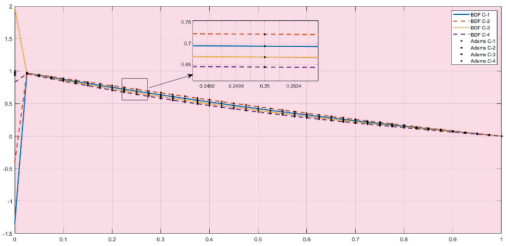

FiG.3-b

Solution graph outcomes

$\theta[\zeta]$ →Y-axis

ζ →X-axis

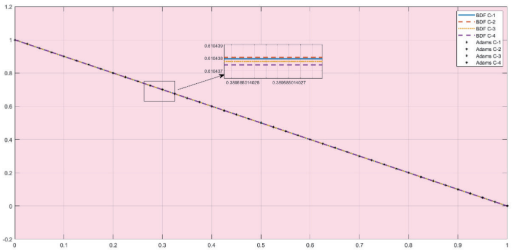

FiG.3-c

Solution graph outcomes

$P[\zeta]$ →Y-axis

ζ →X-axis

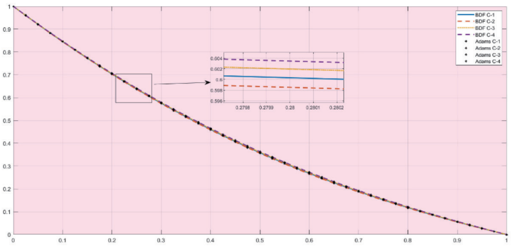

FiG.3-d

Solution graph outcomes

$H[\zeta]$ →Y-axis

ζ → X-axis

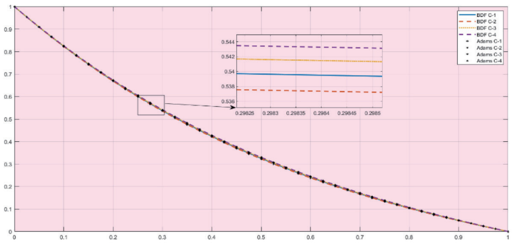

Fig. 3 Comparing the results of Adams and BDF with analysis on solution graphs for MHD-HNF fluidic model for SCN-01 of four cases by varying parameters Kp=1.0, 0.5,1.5,2.

FiG.4-a

Solution graph outcomes

$F'[\zeta]$ →Y-axis

ζ → X-axis

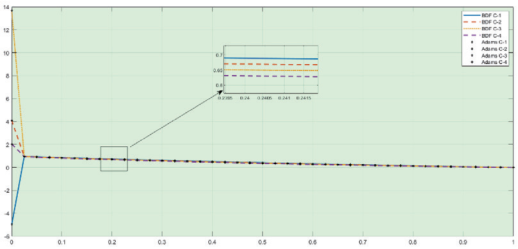

FiG.4-b

Solution graph outcomes

$\theta[\zeta]$ →Y-axis

ζ →X-axis

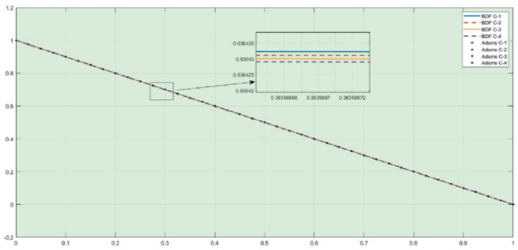

FiG.4-b

Solution graph outcomes

$\theta[\zeta]$ →Y-axis

ζ →X-axis

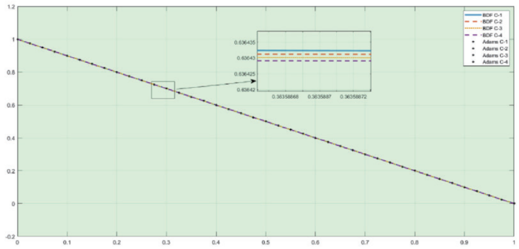

FiG.4-c

Solution graph outcomes

$P[\zeta]$ →Y-axis

ζ →X-axis

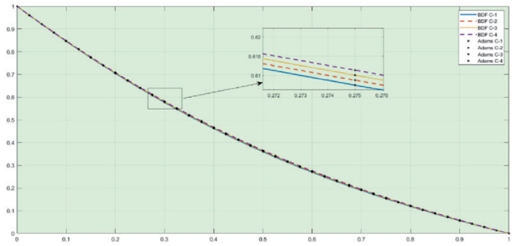

Fig. 4 Comparing the results of Adams and BDF with analysis on solution graphs for MHD-HNF fluidic model for SCN-02 of four cases by varying parameters λ=0.5,1.0,1.5,2.0

FiG.5-a

Solution graph outcomes

$F'[\zeta]$ →Y-axis

ζ → X-axis

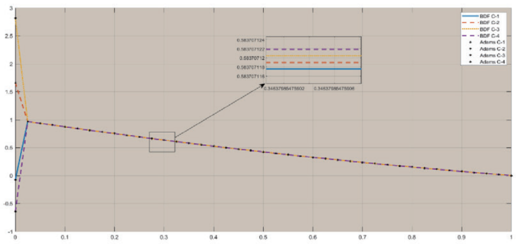

FiG.5-b

Solution graph outcomes

$\theta[\zeta]$ →Y-axis

ζ →X-axis

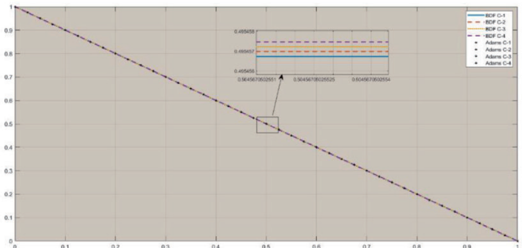

FiG.5-c

Solution graph outcomes

$P[\zeta]$ →Y-axis

ζ →X-axis

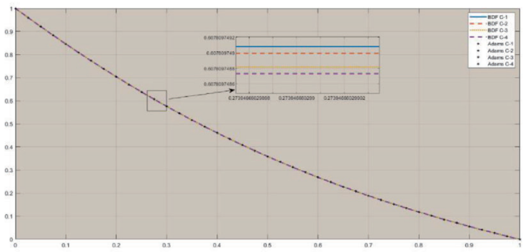

FiG.5-d

Solution graph outcomes

$H[\zeta]$ →Y-axis

ζ → X-axis

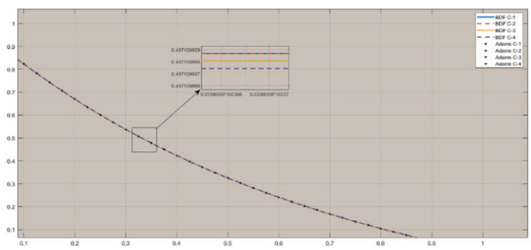

Fig. 5 Comparing the results of Adams and BDF with analysis on solution graphs for MHD-HNF fluidic model for

SCN-03 of four cases by varying parameters Q=0.01,0.02,0.03,0.04

FiG.5-a
Solution graph outcomes
$F'[\zeta]$→Y-axis
ζ → X-axis

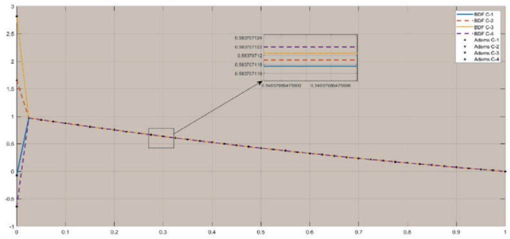

FiG.5-b
Solution graph outcomes
$\theta[\zeta]$→Y-axis
ζ →X-axis

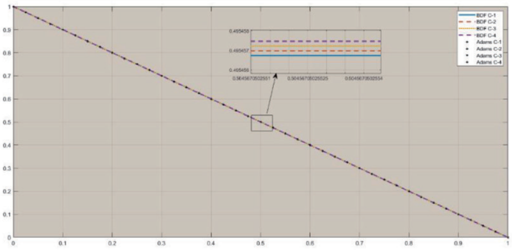

FiG.5-c
Solution graph outcomes
$P[\zeta]$→Y-axis
ζ →X-axis

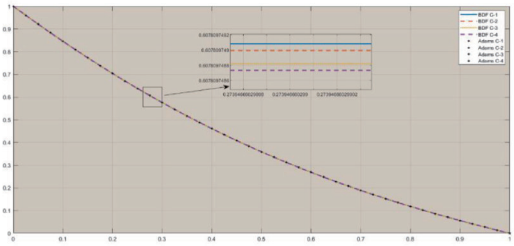

FiG.5-d
Solution graph outcomes
$H[\zeta]$ →Y-axis
ζ → X-axis

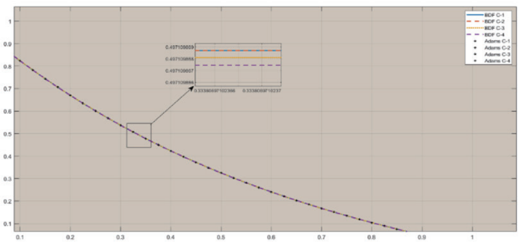

Fig. 6 Comparing the results of Adams and BDF with analysis on solution graphs for MHD-HNF fluidic model for SCN-04 of four cases by varying parameters Ec=0.1,0.2,0.3,0.4

FiG.7-a
Absolute error results
$F'[\zeta]$→ Y-axis
ζ → X-axis

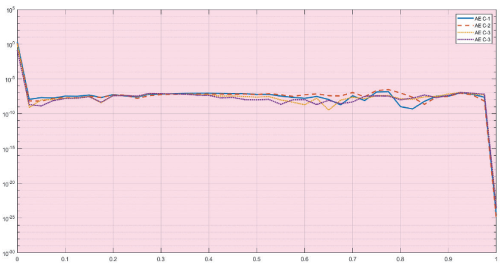

FiG.7-b
Absolute error results
$\theta[\zeta]$→Y-axis
ζ →X-axis

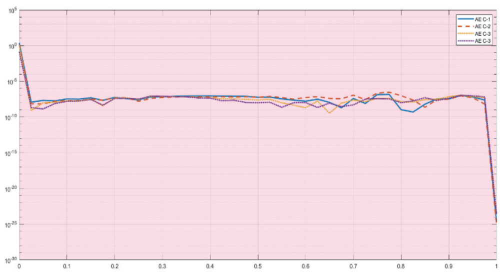

FiG.7-c
Absolute error results
$P[\zeta]$→Y-axis
ζ →X-axis

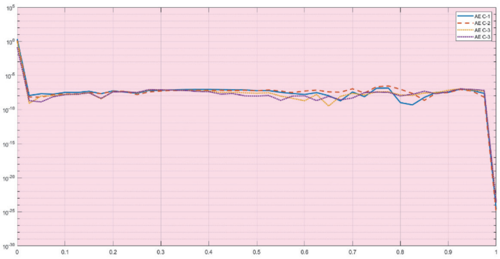

FiG.7-d
Absolute error results
$H[\zeta]$ →Y-axis
ζ → X-axis

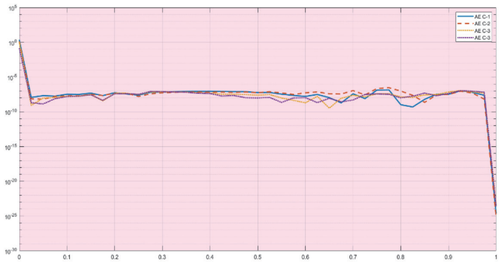

Fig. 7 Comparing the results of Adams and BDF with analysis on Absolute error for MHD-HNF fluidic model for SCN-01 of four cases by varying parameter, Kp=1.0, 0.5,1.5,2.0

5. CONCLUSION

The current study explores the novel bioconvective characteristics of magnetohydrodynamics (MHD-HNF) hybrid nanofluidic flow. This flow comprises colloidal nanoparticles of MgO-Cu flowing through an expanding permeable membrane or sheet. Physical elements such as Eckert number, heat generation, viscous dissipation and buoyancy influences are included. Additionally, the occurrence of microorganisms contributes to the fluid stability.

Water serves as the base fluid, while copper and magnesium oxide are the colloidal nanoparticles. The study analyzes the impact of heat generation and temperature on the fluid flow. Mathematical partial differential equations (PDEs) are simplified into an ordinary(standard) differential equations (ODE) system using non-dimensional parameters and similarity transformations. We obtain distinct values of the governing parameters using the Adams numerical method and the Backward Differential formula (BDF) method by numerical solutions.

The predicted and actual findings from these methods are converted to MATLAB. Absolute error and solution graphs are compared, establishing a strong agreement with the previously published research. Through comprehensive parametric investigation, the effects of physical factors such as velocity, temperature, concentration and microorganisms are explored. Mutual influences are illustrated graphically and numerical comparisons are presented in tabular form.

In conclusion, this study successfully investigates the bioconvective characteristics of MHD-HNF hybrid nanofluidic flow, validating the numerical methods used and highlighting the impact of different physical parameters on fluidic behavior.

REFERENCES

[1] Bognár, G., Klazly, M. and Hriczó, K., 2020. "Nanofluid flow past a stretching plate." *Processes*, **8**(7), p.827.
[2] Chen, C.H., 2003. "Heat transfer in a power-law fluid film over

a unsteady stretching sheet." *Heat and Mass transfer*, **39**(8), pp.791-796.

[3] De Vicente, J., López-López, M.T., González-Caballero, F. and Durán, J.D.G., 2003. "Rheological study of the stabilization of magnetizable colloidal suspensions by addition of silica nanoparticles." *Journal of rheology*, **47**(5), pp.1093-1109.

[4] Dékány, I., Turi, L., Szücs, A. and Király, Z., 1998. "Preparation of semiconductor and transition metal nanoparticles on colloidal solid supports." *Colloids and Surfaces A: Physicochemical and Engineering Aspects*, **141**(3), pp.405-417.

[5] Sidik, N.A.C., Jamil, M.M., Japar, W.M.A.A. and Adamu, I.M., 2017. "A review on preparation methods, stability and applications of hybrid nanofluids." *Renewable and Sustainable Energy Reviews*, **80**, pp.1112-1122.

[6] Hentschke, R., 2016. "On the specific heat capacity enhancement in nanofluids. " Nanoscale research letters, 11, pp.1-11.

[7] De Castro, C.N., Murshed, S.S., Lourenço, M.J.V., Santos, F.J.V., Lopes, M.M. and França, J.M.P., 2012. "Enhanced thermal conductivity and specific heat capacity of carbon nanotubes ionanofluids." *International Journal of Thermal Sciences*, **62**, pp.34-39.

[8] Chereches, E.I., Prado, J.I., Ibanescu, C., Danu, M., Minea, A.A. and Lugo, L., 2020. "Viscosity and isobaric specific heat capacity of alumina nanoparticle enhanced ionic liquids: An experimental approach." *Journal of Molecular Liquids*, **317**, p.114020.

[9] Khanafer, K. and Vafai, K., 2019. "Applications of nanofluids in porous medium: a critical review." *Journal of Thermal Analysis and Calorimetry*, **135**, pp.1479-1492.

[10] Bourantas, G.C., Skouras, E.D., Loukopoulos, V.C. and Burganos, V.N., 2014. "Heat transfer and natural convection of nanofluids in porous media." *European Journal of Mechanics-B/Fluids*, **43**, pp.45-56.

[11] Roy, N.C. and Pop, I., 2020. "Flow and heat transfer of a second-grade hybrid nanofluid over a permeable stretching/shrinking sheet." *The European Physical Journal Plus*, **135**(9), p.768.

[12] Nadeem, M., Siddique, I., Awrejcewicz, J. and Bilal, M., 2022. "Numerical analysis of a second-grade fuzzy hybrid nanofluid flow and heat transfer over a permeable stretching/shrinking sheet." *Scientific Reports*, **12**(1), p.1631.

[13] Sunthrayuth, P., Abdelmohsen, S.A., Rekha, M.B., Raghunatha, K.R., Abdelbacki, A.M., Gorji, M.R. and Prasannakumara, B.C., 2022. " Impact of nanoparticle aggregation on heat transfer phenomena of second grade nanofluid flow over melting surface subject to homogeneous-heterogeneous reactions. " *Case Studies in Thermal Engineering*, **32**, p.101897.

[14] Reddy, P.S. and Chamkha, A.J., 2016. "Influence of size, shape, type of nanoparticles, type and temperature of the base fluid on natural convection MHD of nanofluids." *Alexandria Engineering Journal*, **55**(1), pp.331-341.

[15] Khan, L.A., Raza, M., Mir, N.A. and Ellahi, R., 2020. "Effects of different shapes of nanoparticles on peristaltic flow of MHD nanofluids filled in an asymmetric channel: a novel mode for heat transfer enhancement." *Journal of Thermal Analysis and Calorimetry*, **140**, pp.879-890.

[16] Rashidi, M.M., Kavyani, N. and Abelman, S., 2014. "Investigation of entropy generation in MHD and slip flow over a rotating porous disk with variable properties." *International Journal of Heat and Mass Transfer*, **70**, pp.892-917.

[17] Malik, M.Y., Hussain, A., Salahuddin, T., Awais, M., Bilal, S. and Khan, F., 2016. "Flow of Sisko fluid over a stretching cylinder and heat transfer with viscous dissipation and variable thermal conductivity: a numerical study." *AIP Advances*, **6**(4).

[18] Khan, W.A., 2022. "Numerical simulation of Chun-Hui He's iteration method with applications in engineering." *International Journal of Numerical Methods for Heat & Fluid Flow*, **32**(3), pp.944-955.

[19] Khan, W.A., 2021. "Numerical and simulation analysis comparison of hydraulic network problem base on higher-order efficiency approach." *Alexandria Engineering Journal*, **60**(5), pp.4889-4903.

[20] Suresh, S., Venkitaraj, K.P., Selvakumar, P. and Chandrasekar, M., 2011. "Synthesis of Al2O3–Cu/water hybrid nanofluids using two step method and its thermo physical properties. " *Colloids and Surfaces A: Physicochemical and Engineering Aspects*, **388**(1-3), pp.41-48.

[21] Syam Sundar, L., Sousa, A.C. and Singh, M.K., 2015. "Heat transfer enhancement of low volume concentration of carbon nanotube-Fe3O4/water hybrid nanofluids in a tube with twisted tape inserts under turbulent flow." *Journal of Thermal Science and Engineering Applications*, **7**(2), p.021015.

[22] Nabil, M.F., Azmi, W.H., Hamid, K.A., Zawawi, N.N.M., Priyandoko, G. and Mamat, R., 2017. "Thermo-physical properties of hybrid nanofluids and hybrid nanolubricants: a comprehensive review on performance." *International Communications in Heat and Mass Transfer*, **83**, pp.30-39.

[23] Javid, K., Ali, N. and Bilal, M., 2020. "A numerical simulation of the creeping flow of hybrid-nano-fluid through a curved configuration due to metachronal waves propulsion of beating cilia". *The European Physical Journal Plus*, **135**(1), p.49.

[24] Fallah, B., Dinarvand, S., Eftekhari Yazdi, M., Rostami, M.N. and Pop, I., 2019. "MHD flow and heat transfer of SiC-TiO2/DO hybrid nanofluid due to a permeable spinning disk by a novel algorithm." *Journal of Applied and Computational Mechanics*, **5**(5), pp.976-988.

[25] Rafique, K., Mahmood, Z. and Khan, U., 2023. "Mathematical analysis of MHD hybrid nanofluid flow with variable viscosity and slip conditions over a stretching surface." *Materials Today Communications*, **36**, p.106692.

[26] Shamshuddin, M.D., Salawu, S.O., Ramesh, K., Patil, V.S. and Humane, P., 2023. "Bioconvective treatment for the reactive Casson hybrid nanofluid flow past an exponentially stretching sheet with Ohmic heating and mixed convection." *Journal of Thermal Analysis and Calorimetry*, **148**(21), pp.12083-12095.

[27] Sankari, M.S., Rao, M.E., Khan, W., Makinde, O.D., Chamkha, A.J. and Salah, B., 2024. "Homotopic analysis for bioconvection of Casson nanofluid flow over an exponential stretching sheet with activation energy and motile microorganism." *Numerical Heat Transfer, Part A: Applications*, pp.1-23.

[28] Humane, P.P., Patil, V.S., Shamshuddin, M.D., Rajput, G.R. and

Patil, A.B., 2023. “Role of bioconvection on the dynamics of chemically active Casson nanofluid flowing via an inclined porous stretching sheet with convective conditions.” *International Journal of Modelling and Simulation*, pp.1-20.

[29] Joshi, N., Upreti, H. and Pandey, A.K., 2022. “MHD Darcy-Forchheimer Cu-Ag/H2O-C2H6O2 hybrid nanofluid flow via a porous stretching sheet with suction/blowing and viscous dissipation.” *International Journal for Computational Methods in Engineering Science and Mechanics*, **23**(6), pp.527-535.

[30] Rashid, A., Ayaz, M., Islam, S., Saeed, A., Kumam, P. and Suttiarporn, P., 2022. “Theoretical analysis of the MHD flow of a tangent hyperbolic hybrid nanofluid over a stretching sheet with convective conditions: a nonlinear thermal radiation case. ” *South African Journal of Chemical Engineering*, **42**, pp.255-269.

[31] Mumtaz, M., Islam, S., Ullah, H. and Shah, Z., 2023. “Chemically reactive MHD convective flow and heat transfer performance of ternary hybrid nanofluid past a curved stretching sheet.” *Journal of Molecular Liquids*, *390*, p.123179.

[32] Waqas, H., Farooq, U., Liu, D., Abid, M., Imran, M. and Muhammad, T., 2022. “Heat transfer analysis of hybrid nanofluid flow with thermal radiation through a stretching sheet: A comparative study.” *International Communications in Heat and Mass Transfer*, **138**, p.106303.

[33] Shehzad, S.A., Hayat, T., Qasim, M. and Asghar, S., 2013. “Effects of mass transfer on MHD flow of Casson fluid with chemical reaction and suction.” *Brazilian journal of chemical engineering*, **30**, pp.187-195.

[34] Parveen, N., Awais, M. and Awan, S.E., 2024. “Generalized thermal properties of hybrid NANOLIQUID composed of aluminum oxide (Al2O3) and silver (Ag) nanoparticles with water (H2O) as base liquid.” *ZAMM-Journal of Applied Mathematics and Mechanics/Zeitschrift für Angewandte Mathematik und Mechanik*, **104**(1), p.e202300194.

[35] Neethu, T.S., Sabu, A.S., Mathew, A., Wakif, A. and Areekara, S., 2022. “Multiple linear regression on bioconvective MHD hybrid nanofluid flow past an exponential stretching sheet with radiation and dissipation effects.” *International Communications in Heat and Mass Transfer*, **135**, p.106115

[36] Awan, S.E., Awais, M., Raja, M.A.Z., Parveen, N., Ali, H.M., Khan, W.U. and He, Y., 2021. “Numerical treatment for dynamics of second law analysis and magnetic induction effects on ciliary induced peristaltic transport of hybrid nanomaterial.” *Frontiers in Physics*, **9**, p.631903.

[37] Farooq, U., Hussain, M., Ijaz, M.A., Khan, W.A. and Farooq, F.B., 2021. “Impact of non-similar modeling on Darcy-Forchheimer-Brinkman model for forced convection of Casson nano-fluid in non-Darcy porous media.” *International Communications in Heat and Mass Transfer*, **125**, p.105312.